Published in final edited form as:
Lipids. 2005 May ; 40(5): 495–500.

Lipid Composition Influences the Shape of Human Low-Density Lipoprotein in Vitreous Ice

Andrea Coronado-Gray and **Rik van Antwerpen***

Department of Biochemistry, Medical College of Virginia Campus, Virginia, Commonwealth University, Richmond, Virginia 23298, USA

Abstract

Earlier cryo-electron microscopic studies have indicated that the normal low-density lipoprotein (N-LDL) has a discoid shape when its core is in the liquid-crystalline state. In the present study, we investigated whether the shape of LDL depends on the physical state and/or the lipid composition of the lipoprotein core. Using a custom-built freezing device, we vitrified N-LDL samples from either above or below the phase-transition temperature of the core (42°C and 24°C, respectively). Cryo-electron microscopy revealed no differences between these samples and indicated a discoid shape of the N-LDL particle. In contrast, triglyceride-enriched LDL (T-LDL) did not have discoid features and appeared to be quasi-spherical in preparations that were vitrified from either 42°C or 24°C. These results suggest that the shape of N-LDL is discoid, regardless of the physical state of its core, while T-LDL is more spherical. Aspects that may influence the shape of LDL are discussed.

Keywords

structure; electron microscopy; differential scanning calorimetry; phase-transition; physical state

Abbreviations:

apoB apolipoprotein B-100; cryo-EM cryo-electron microscopy; DSC differential scanning calorimetry; LDL low-density lipoprotein; N-LDL normal low-density lipoprotein; T-LDL triglyceride-rich low-density lipoprotein

The low-density lipoprotein (LDL) transports cholesterol throughout the human body, and elevated levels of this lipoprotein in the blood correlate with increased risk of atherosclerosis and coronary heart disease. LDL is a quasi-spherical particle, that contains a core of mainly cholesteryl esters and a surface monolayer of phospholipids, free cholesterol, and a single molecule of apolipoprotein B-100 (apoB; M_r ~550,000) (1,2). ApoB is a ligand for the apoB/E-receptor, allowing for receptor-mediated endocytosis of LDL by cells that express the receptor (3,4). In addition, apoB binds to proteoglycans in the vascular wall (5,6), which is one of the critical first steps in atherosclerosis (7,8). Thus, both the normal metabolism of LDL and the pathogenic properties of the lipoprotein particle depend on the structure of apoB.

Studies have shown that the lipid composition and size of the LDL core influence the conformation of apoB on the lipoprotein surface. Structural parameters, such as the relative amount of α-helical and β-sheet structure (9,10), the exposure of lysine amino groups on the LDL surface (11), the exposure of epitopes on the LDL surface (10–12), the susceptibility of

* Address correspondence to: Rik van Antwerpen, Department of Biochemistry, Medical College of Virginia Campus, Virginia Commonwealth University, P.O. Box 980614, Richmond, Virginia 23298, USA. Telephone: 804-828-3509; Fax: 804-828-1473; E-mail: hgvanant@hsc.vcu.edu.

apoB to protease digestion (9), and the affinity of apoB for the LDL receptor (9–12,13,14), all depend on the size of the LDL core. As a result, small dense LDL particles appear to be more atherogenic than larger and more buoyant LDL (15,16).

Recent experiments have shown that the conformation of apoB on the LDL surface also depends on the physical state of the LDL core (17,18). The main components of the core, cholesteryl esters, are normally in a disordered, liquid state at physiological temperature and in a more ordered, liquid-crystalline state at room temperature (19–25). The temperature at which the transition between these two states occurs, i.e., the phase-transtion temperature, is usually around 30°C. However, animal studies have shown that diets with a high content of cholesterol and saturated fat can change the composition of the LDL core, and as a result elevate the phase-transition temperature to 40–45°C (26–28). Temperature-dependent infrared spectroscopy and circular dichroism studies (17,18) indicate that these diet-induced changes in the physical state of the core may affect the conformation of apoB on the LDL surface, which, in turn, may influence the metabolic and pathogenic properties of the lipoprotein particle.

Recent cryo-electron microscopy (cryo-EM) studies have shown quite unexpectedly that LDL particles with a liquid-crystalline core may have an oblate ellipsoid or “discoid” shape (29–34). Low-resolution X-ray crystallography and high-performance gel-filtration chromatography appear to confirm the discoid nature of the LDL complex (35,36). Based on these observations, we have recently speculated that the liquid to liquid-crystalline transition of the LDL core may be associated with a spherical to discoid change in the shape of the lipoprotein particle, and that this shape change may be responsible for the observed change in the conformation of apoB on the LDL surface (18,33). A recent cryo-EM study seems to confirm this suggestion (34), however, high-performance gel-filtration chromatography indicates that LDL has a discoid shape regardless of the physical state of its core (36).

To address this issue further, we analysed two LDL species with different core properties using cryo-EM. Our results suggest that the shape of normal LDL is discoid, regardless of the physical state of its core, and that triglyceride-rich LDL is more spherical.

MATERIALS AND METHODS

LDL Samples

Normal LDL (N-LDL), d = 1.019 – 1.064 g/ml, was isolated from the blood of a healthy, non-smoking, normolipidemic donor, using sequential floatation ultracentrifugation as described earlier (18). Triglyceride-enriched LDL (T-LDL) was produced by an *in vitro* lipid transfer procedure, using N-LDL, Intralipid (Sigma Chemical Company, St. Louis, MO), and lipoprotein-deficient plasma as a source for cholesteryl ester transfer protein (18). The integrity of apoB in N-LDL and T-LDL was confirmed using sodium dodecyl sulfate polyacrylamide gel electrophoresis according to Leammli (37). Protein concentrations were determined with a modified Lowry assay, using bovine serum albumin as a standard (38). Total cholesterol concentrations were determined using assay kit 439-17501 from Wako Chemicals (Richmond, VA). Triglyceride concentrations were determined using assay kit TR22421 from Thermo Trace (Melbourne, Australia).

Differential Scanning Calorimetry (DSC)

DSC was performed using a Nano II Differential Scanning Calorimeter (Calorimetry Sciences Corporation, American Fork, UT). Before analysis, LDL samples were dialyzed into 10 mM sodium phosphate buffer (pH 7.4). Buffer and LDL samples were degassed under vacuum, after which 0.6 ml of each was loaded into the reference and sample cells of the calorimeter,

respectively. LDL samples were analyzed at protein concentrations of 0.75 – 1.5 mg/ml. Thermograms were recorded over a temperature range of 0–45°C at heating and cooling rates of 60°C/h . Three sequential up- and down-scans were performed to verify reversibility of the phase-transition.

Preparation of LDL for cryo-EM

Cryo-EM samples were prepared with a custom-built freezing device as described in Figure 1. Using this device, LDL samples were vitrified either from 24°C or from 42°C. Before loading into the freezing device, samples were incubated for at least 15 min in a temperature-controlled waterbath in order to bring the preparations to the desired temperature (either 24°C or 42°C). Once the samples were loaded into the freezing device, they were equilibrated at the desired temperature for an additional 5 min before plunge-freezing. These loading procedures assured that the LDL sample was either at 24°C or at 42°C immediately prior to vitrification.

Vitrification, i.e., freezing at rates that are high enough to prevent the formation of ice crystals, is commonly achieved when thin cryo-EM samples are plunged into liquid propane or ethane (29–31,39). Earlier studies have shown that the vitrification process is fast enough to capture membrane fusion intermediates and characteristic features of lipid phases that exist above the phase-transition temperature of the system (40–42). The present study, therefore, assumes that structural features related to the physical state of the LDL core are, likewise, preserved during vitrification.

Cryo-electron microscopy

N-LDL and T-LDL samples were analyzed under low-dose conditions, at 120 kV and −170° C, using a JEOL 1200EX electron microscope (JEOL, Ltd., Peabody, MA) and a Gatan model 626 cryo-transfer device (Gatan, Inc., Warendale, PA), as described earlier (29–31). The following areas of the preparation were exluded from analysis: 1) Areas in which the ice was too thick for penetration of the electron beam. 2) Areas with cubic or hexagonal ice crystals. These ice crystals, which prevent proper structural analysis, are easily recognized in electron diffraction patterns (in the electron microscope) and in the final cryo-EM image (photographic negative). 3) Areas in which the ice was too thin for random orientation of the LDL particles. These areas did not appear very often, and can be recognized by a steep gradient of background ice combined with altered distribution of various projections (43). All other areas of the cryo-EM preparation were photographed and included in the analysis. At least 500 projections of each sample were measured. Images were recorded on Kodak 4489 film (Eastman Kodak Company, Rochester, NY), at a magnification 30,000x. Photographic negatives were digitized at an optical resolution of 4800 dpi, using a FlexTight Prescision II Scanner (Imacon, Inc., Redmond, WA). Dimensions of the various LDL projections were determined using the measuring tool of Adobe Photoshop, software version 5.0 (Adobe Systems, Inc., San Jose, CA.

RESULTS

The influence of the physical state and lipid composition of the LDL core on the overall shape and substructure of the lipoprotein particle was analyzed with two different LDL species: normal LDL (N-LDL), with a core phase-transition temperature of ~31°C, and *in-vitro*-produced triglyceride-rich LDL (T-LDL) with a core phase-transition temperature of ~15°C (Fig. 2). The cholesterol and triglyceride content, as well as some of the physical properties of these two LDL species, are shown in table 1.

N-LDL samples vitrified from 24°C or 42°C

Figure 3A shows a typical N-LDL preparation that was vitrified from 24°C (which is ~7°C below the phase-transition temperature of the N-LDL core). Various types of projections of

the LDL structure are observed, including circular projections with a high-density ring, and rectangular projections with two high-density bands. Earlier studies have shown that these projections represent face-on and edge-on views of a discoid structure, respectively (29–31). The projection most indicative of the discoid shape of N-LDL is the rectangular projection, resulting from an edge-on view of the structure. However, as the lipoprotein particles are free to rotate in solution immediately prior to vitrification, only a limited number of particles provides an edge-on view. In N-LDL preparations vitrified from 24°C, 12.8% of all measured projections was unambiguously rectangular with two high-density bands (Fig. 4). This is in good agreement with the number of rectangular projections observed in previous studies (29–31).

Figure 3B shows a typical N-LDL preparation that was vitrified from 42°C (which is ~11°C above the phase-transition temperature of the N-LDL core). Like in preparations vitrified from 24°C, various types of projections of the LDL structure are observed, including circular projections with a high-density ring, and rectangular projections with two high-density bands. The various projections observed in preparations frozen from 42°C were indistinguishable from those observed in preparations frozen from 24°C. In N-LDL preparations vitrified from 42°C, 10.2% of all measured projections was unambiguously rectangular with two high-density bands (Fig. 4). This percentage not significantly different from the percentage of rectangular projections seen in N-LDL preparations frozen from 24°C (Fig. 4), indicating that, like at 24°C, N-LDL has a discoid shape at 42°C.

T-LDL samples vitrified from 24°C or 42°C

T-LDL samples were vitrified from 24°C and 42°C to further assess whether LDL particles with a liquid core have discoid features. As the phase-transition temperature of the T-LDL core is ~15°C, T-LDL has a liquid core at both experimental temperatures. Figures 3C and 3D show typical cryo-EM preparations of T-LDL, vitrified from 24°C and 42°C, respectively. In both types of T-LDL preparations, very few rectangular projections with two high density bands were observed. In T-LDL preparations frozen from 24°C, only 0.8% of the measured projections was rectangular, while in preparations frozen from 42°C, 0.5% of the measured projections was rectangular (Fig. 4). These observations indicate that T-LDL particles are not discoid, but instead, have a more sperical shape. The fact that N-LDL with a liquid core, vitrified from 42°C, has a discoid shape (see above), suggests that the high triglyceride content of the T-LDL core, not the physical state of the core, is responsible for the quasi-spherical features of T-LDL (Table 2).

DISCUSSION

Molecular models of LDL generally depict the lipoprotein particle as a sphere. In these models, the liquid-crystalline LDL core is organized in concentric, spherical layers of cholesteryl esters (19–25) (Fig. 5A). However, recent cryo-EM studies suggest that LDL has an oblate ellipsoid, or discoid shape when its core is in the liquid-crystalline state (29–34). This suggestion has recently been supported by low-resolution X-ray crystallography (35) and high-performance gel-filtration chromatography (36). New LDL models, therefore, propose that the liquid-crystalline core is organized in flat layers of cholesteryl esters (32,35,36) (Fig. 5B), which is consistent with the crystallization of neat cholesteryl esters in flat sheets (44).

The present study was designed to test the hypothesis that the phase-transition of the LDL core is associated with a spherical-to-discoid change in the shape of the lipoprotein particle. Quite unextectedly, projections of N-LDL in preparations vitrified from 42°C (i.e., ~11°C above the phase-transition of the LDL core) (Fig. 3B) are similar those observed in preparations vitrified from 24°C (i.e., ~7°C below the phase-transition of the LDL core) (Fig. 3A). In addition, roughly equal numbers of rectangular projections, representing edge-on views of the discoid

structure (29–31), are observed in preparations vitrified from 42°C or 24°C (Fig. 4). These results suggest that the N-LDL particle has a discoid shape regardless of the physical state of its core.

Our present results are in agreement with a recent study by Teerlink *et al.* (36), who used compositional analyses in combination with high-performance gel-filtration chromatography to investigate the shape of LDL. Their results fit a discoid model of LDL better than a spherical model, both at 24°C, when the core is liquid-crystalline, and at 37°C, when the core is liquid. Interestingly, however, our results seem to disagree with a recent cryo-EM study by Sherman *et al.* (34), suggesting that LDL particles with a liquid core are spherical. The reason for this discrepancy is not clear. However, we have recently observed that discoid LDL particles may assume preferred face-on orientations in extremely thin aqueous films, resulting in a predominance of circular projections on the microscope screen (43). This predominance of circular projections may create the impression that the LDL particle has a spherical shape, while, in fact, only face-on orientations of a discoid structure are observed.

The present study shows that triglyceride-rich LDL (T-LDL) does not have discoid features, indicating that the triglyceride content of the LDL core plays a role in determining the shape of LDL. Consistent with this suggestion is the cryo-EM observation that triglyceride-rich very-low-density lipoproteins and intermediate-density lipoproteins (IDLs) are spherical, while IDL particles with a lower triglyceride content are discoid in preparations that are vitrified from room temperature (31). In addition, similar to T-LDL in the present study, triglyceride-rich small dense LDL from hypertriglyceridemic subjects lacks discoid features (30). A possible explanation for the absence of discoid features in triglyceride-rich lipoprotein particles may be found in a recent study by Pregetter *et al.* (45). The authors of this study propose that, below the phase transition temperature, the core of triglyceride-rich LDL contains two concentric compartments: a fluid inner-core containing mostly triglycerides, surrounded by a shell of cholesteryl esters in the liquid-crystalline state. Thus, the presence of a relatively large triglyceride inner-core may prevent the arrangement of cholesteryl esters in flat layers.

Presently, it can not be excluded that the discoid shape of normal LDL, observed with cryo-EM (29–34), X-ray crystallography (35), and high-performance gel-filtration chromatography (36), is generated during isolation or storage of the lipoprotein complex at non-physiological temperatures, i.e., below the phase-transition of the cholesteryl ester core. These conditions may irreversibly deform the shape of LDL, which, in the native state, may still be spherical. It will be important to resolve this issue while attempts are made to reconstruct the three-dimensional structure of LDL at higher resolution.

Acknowledgements

The authors thank Dr. John C. Gilkey for stimulating discussions, Ms. Iris Davis at the VCU Office of Employee Health Servives for drawing blood samples, and Ms. Wilma Espiritu for technical assistance. This work was supported by a pre-doctoral fellowship of the National Heart Lung and Blood Institute to Andrea Coronado-Gray (HL69741), and by grants from the American Heart Association (AZGB3097) and the National Heart, Lung, and Blood Institute (HL67402).

References

1. Hevonoja T, Pentikäinen MO, Hyvönen MT, Kovanen PT, Ala-Korpela M. Structure of Low Density Lipoprotein (LDL) Particles: Basis for Understanding Molecular Changes in Modified LDL. Biochim Biophys Acta 2000;1488:189–210. [PubMed: 11082530]
2. Segrest JP, Jones MK, De Loof H, Dashti N. Structure of Apolipoprotein B-100 in Low Density Lipoproteins. J Lipid Res 2001;42:1346–1367. [PubMed: 11518754]
3. Borén J, Lee I, Zu W, Arnold K, Taylor S, Innerarity T. Identification of the Low Density Lipoprotein Receptor-Binding Site in Apolipoprotein B100 and the Modulation of its Binding Activity by the

Carboxyl Terminus in Familial Defective Apo-B100. J Clin Invest 1998;101:1084–1093. [PubMed: 9486979]

4. Borén J, Ekström U, Ågren B, Nilsson-Ehle P, Innerarity TL. The Molecular Mechanism for the Genetic Disorder Familial Defective Apolipoprotein B100. J Biol Chem 2001;276:9214–9218. [PubMed: 11115503]
5. Borén J, Olin K, Lee I, Chait A, Wight TN, Innerarity TL. Identification of the Principal Proteoglycan Binding Site in LDL. A Single Point Mutation in Apo-B100 Severely Affects Proteoglycan Interaction Without Affecting LDL Receptor Binding. J Clin Invest 1998;101:2658–2664. [PubMed: 9637699]
6. Goldberg IJ, Wagner WD, Pang L, Paka L, Curtiss LK, DeLozier JA, Shelness GS, Young CSH, Pillarisetti S. The NH_2-terminal Region of Apolipoprotein B Is Sufficient for Lipoprotein Association with Glycosaminoglycans. J Biol Chem 1998;273:35355–35361. [PubMed: 9857078]
7. Camejo G, Hurt-Camejo E, Wiklund O, Bondjers G. Association of Apo B Lipoproteins with Arterial Proteoglycans: Pathological Significance and Molecular Basis. Atherosclerosis 1998;139:205–222. [PubMed: 9712326]
8. Boren J, Gustafsson M, Skalen K, Flood C, Innerarity TL. Role of Extracellular Retention of Low Density Lipoproteins in Atherosclerosis. Curr Opinion Lipidol 2000;11:451–456.
9. Chen GC, Liu W, Duchatteau P, Allaart J, Hamilton RL, Mendel CM, Lau K, Hardman DA, Frost PH, Malloy MJ, Kane JP. Conformational Differences in Human Apolipoprotein B-100 Among Subspecies of Low Density Lipoproteins (LDL). Association of Altered Proteolytic Accessibility with Decreased Receptor Binding of LDL Subspecies from Hypertriglyceridemic Subjects. J Biol Chem 1994;269:29121–29128. [PubMed: 7961878]
10. Galeano NF, Milne R, Marcel YL, Walsh MT, Levy E, Ngu'yen T-D, Gleeson A, Arad Y, Witte L, Al-Haideri M, Rumsey SC, Deckelbaum RJ. Apoprotein B Structure and Receptor Recognition of Triglyceride-Rich Low Density Lipoprotein (LDL) is Modified in Small LDL But Not in Triglyceride-Rich LDL of Normal Size. J. Biol. Chem 1994;269:511–519.48. [PubMed: 8276844]
11. Aviram M, Lund-Katz S, Phillips MC, Chait A. The Influence of the Triglyceride Content of Low Density Lipoprotein on the Interaction of Apolipoprotein B-100 with Cells. J. Biol. Chem 1988;263:16842–16848.49. [PubMed: 3182816]
12. McKeone BJ, Patsch JR, Pownall HJ. Plasma Triglycerides Determine Low Density Lipoprotein Composition, Physical Properties, and Cell-Specific Binding in Cultured Cells. J Clin Invest 1993;91:1926–1933. [PubMed: 8387537]
13. De Graaf J, Hendriks JC, Swinkels DW, Demacker PN, Stalenhoef AF. Differences in LDL Receptor-Mediated Metabolism of Three Low Density Lipoprotein Subfractions by Human Monocyte-Derived Macrophages: Impact on the Risk of Atherosclerosis. Artery 1993;20:201–230. [PubMed: 8250739]
14. Campos H, Arnold KS, Balestra ME, nnerariry TL, Krauss RM. Differences in Receptor Binding of LDL Subfractions. Arterioscler Thromb Vasc Biol 1996;16:794–801. [PubMed: 8640407]
15. Austin MA, Breslow JL, Hennekens CH, Buring JE, Willet WC, Krauss RM. Low-Density Lipoprotein Subclass Patterns and Risk for Myocardial Infarction. JAMA 1988;260:1917–9121. [PubMed: 3418853]
16. Krauss RM. Heterogeneity of Plasma Low-Density Lipoproteins and Atherosclerosis Risk. Curr Opinion Lipidol 1994;5:339–349.
17. Bañuelos S, Arrondo JLR, Goñi FM, Pifat G. Surface-Core Relationships in Human Low Density Lipoprotein as Studied by Infrared Spectroscopy. J Biol Chem 1995;270:9192–9196. [PubMed: 7721835]
18. Coronado-Gray A, Van Antwerpen R. The Physical State of the LDL Core Influences the Conformation of Apolipoprotein B-100 on the Lipoprotein Surface. FEBS Letters 2003;533:21–24. [PubMed: 12505152]
19. Deckelbaum RJ, Shipley GG, Small DM, Lees RS, George PK. Thermal Transition in Human Plasma Low Density Lipoprotteins. Science 1975;190:392. [PubMed: 170681]
20. Atkinson D, Deckelbaum RJ, Small DM, Shipley GG. Structure of Human Plasma Low-Density Lipoproteins: Molecular Organization of the Central Core. Proc Natl Acad Sci USA 1977;74:1043–1046.
21. Deckelbaum RJ, Shipley GG, Small DM. Structure and Interactions of Lipids in Human Plasma Low Density Lipoproteins. J Biol Chem 1977;252:744–754. [PubMed: 188825]

22. Müller K, Laggner P, Glatter O, Kostner G. The Structure of Human-Plasma Low-Density Lipoprotein B. An X-Ray Small-Angle Scattering Study. Eur J Biochem 1978;82:73–90. [PubMed: 202466]

23. Laggner P, Muller KW. The Structure of Serum Lipoproteins as Analysed by X-Ray Small-Angle Scattering. Quart Rev Biophys 1978;11:371–425.

24. Atkinson D, Small DM, Shipley GG. X-ray and Neutron Scattering Studies of Plasma Lipoproteins. Ann NY Acad Sci 1980;348:284–298. [PubMed: 6994563]

25. Laggner P, Kostner GM, Degovics G, Worcester DL. Structure of the Cholesteryl Ester Core of Human Plasma Low Density Lipoproteins: Selective Deuteration and Neutron Small Angle Scattering. Proc Natl Acad Sci USA 1984;81:4389–4393. [PubMed: 6589601]

26. Tall AR, Atkinson D, Small DM, Mahley RW. Characterization of the Lipoproteins of Atherosclerotic Swine. J Biol Chem 1977;252:7288–7293. [PubMed: 198408]

27. Tall AR, Small DM, Atkinson D, Rudel L. Studies on the Structure of Low Density Lipoproteins Isolated From *Macaca Fascicularis* Fed an Atherogenic Diet. J Clin Invest 1978;62:1354–1363. [PubMed: 219029]

28. Parks JS, Bullock BC. Effect of Fish Oil Versus Lard Diets on the Chemical and Physical Properties of Low Density Lipoproteins of Nonhuman Primates. J Lipid Res 1987;28:173–182. [PubMed: 3572246]

29. Van Antwerpen R, Gilkey JC. Cryo-Electron Microscopy Reveals Human Low Density Lipoprotein Substructure. J Lipid Res 1994;35:2223–2231. [PubMed: 7897320]

30. Van Antwerpen R, Chen GC, Pullinger CR, Kane JP, LaBelle M, Krauss RM, Luna-Chavez C, Forte TM, Gilkey JC. Cryo-Electron Microscopy of Low Density Lipoprotein and Reconstituted Discoidal High Density Lipoprotein: Imaging of the Apolipoprotein Moiety. J Lipid Res 1997;38:659–669. [PubMed: 9144081]

31. Van Antwerpen R, La Belle M, Navratilova E, Krauss RM. Structural Heterogeneity of Apolipoprotein B Containing Serum Lipoproteins Visualized Using Cryo-Electron Microscopy. J Lipid Res 1999;40:1827–1836. [PubMed: 10508202]

32. Orlova EV, Sherman MB, Chiu W, Mowri H, Smith LC, Gotto AM Jr. Three-Dimensional Structure of Low Density Lipoproteins by Electron Cryomicroscopy. Proc Natl Acad Sci USA 1999;96:8420–8425. [PubMed: 10411890]

33. Van Antwerpen, R. (2002) Structure of the Low-Density Lipoprotein, LDL. Workshop on Single Particle Reconstructions and Visualization; National Center for Macromolecular Imaging; University of Houston, Houston, Texas, December 11–15, 2002.

34. Sherman MB, Orlova EV, Decker GL, Chiu W, Pownall HJ. Structure of Triglyceride-Rich Human Low-Density Lipoproteins According to Cryo-Electron Microscopy. Biochem 2003;42:14988–14993. [PubMed: 14674775]

35. Lunin VY, Lunina NL, Ritter S, Frey I, Berg A, Diederichs K, Padjarny AD, Urzhumtsev A, Baumstark MW. Low-Resolution Data Analysis for Low-Density Lipoprotein Particle. Acta Cryst D 2001;57:108–121. [PubMed: 11134933]

36. T. Teerlink, Scheffer; P.G., Bakker; S.J.L., Heine; R.J. Combined Data from LDL Composition and Size Measurement Are Compatible with a Discoid Particle Phape. J Lipid Res 2004;45:954–966. [PubMed: 14967822]

37. Laemmli UK. Cleavage of Structural Proteins During the Assembly of the Head of Bacteriophage T4. Nature 1970;227:680–685. [PubMed: 5432063]

38. Peterson GL. Determination of Total Protein. Methods Enzymol 1983;91:95–119. [PubMed: 6855607]

39. Dubochet J, Adrian M, Chang J-J, Homo J-C, Lepault J, McDowall AW, Schultz P. Cryo-Electron Microscopy of Vitrified Specimens. Q Rev Biophys 1988;21:129–228. [PubMed: 3043536]

40. Siegel DP, Burns L, Chesnut H, Talmon Y. Intermediates in Membrane Fusion and Bilayer/Non-Bilayer Phase Transitions Imaged by Time-Resolved Cryo-Transmission Electron Microscopy. Biophys J 1989;56:161–169. [PubMed: 2752086]

41. Frederik PM, Stuart MCA, Bomans PHH, Busing WM, Burger KNJ, Verkleij AJ. Perspective and Limitations of Cryo-Electron Microscopy. From Model Systems to Biological Specimens. J Microsc 1991;161:253–262. [PubMed: 2038033]

42. Siegel DP, Green WJ, Talmon Y. The Mechanism of Lamellar-to-Inverted Hexagonal Phase Transitions: A Study Using Temperature-Jump Cryo-Electron Microscopy. Biophys J 1994;66:402–414. [PubMed: 8161694]

43. Van Antwerpen R. Preferred orientations of LDL in vitreous ice indicate a discoid shape of the lipoprotein particle. Arch Biochem Biophys 2004;432:122–127. [PubMed: 15519303]

44. Ginsburg GS, Atkinson D, Small DM. Physical Properties of Cholesteryl Esters. Prog Lipid Res 1984;23:135–167. [PubMed: 6399750]

45. Pregetter M, Prassl R, Schuster B, Kriechbaum M, Nigon F, Chapman J, Laggner P. Microphase separation in low density lipoproteins; evidence for a fluid triglyceride core below the lipid melting transition. J Biol Chem 1999;274:1334–1341. [PubMed: 9880504]

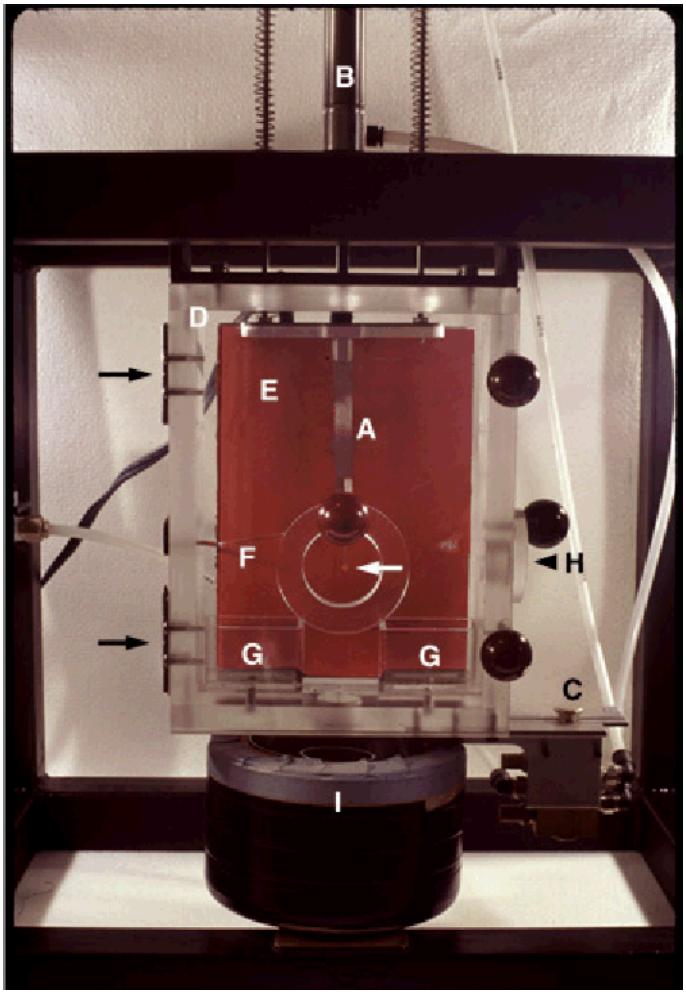

Figure 1.

Custom built freezing device for the vitrification of samples from different temperatures. A pair of forceps (**A**), holding an EM grid with a lacey substrate (**white arrow**), is attached to a plunger (**B**). This plunger is connected to tubing that is pressurized with air. Air pressure in the tubing is adjusted with a control valve (not in the picture), usually set at 20 psi. Release of the pressure with a control switch (**C**) forces the plunger and the attached forceps down with high speed. The environment in the plexiglas box (**D**) can be warmed by a heating pad in the back of the box (**rectangle, E**). Temperature near the EM sample is measured with a thermocouple (**F**) that is connected to a thermostat (not in the picture). In the bottom of the box are two small containers (**G**) that are filled with water. Filter paper soaked with water is guided from the water containers to the top of the heating pad to allow efficient distribution of water vapor throughout the box. The front panel of the box hinges on the left (**black arrows**) and can be opened to allow attachment of the forceps to the plunger and application of sample to the EM grid (**white arrow**). After application of the sample, the front panel is closed and the environment is equilibrated at the desired temperature and high humidity. Subsequently, the bulk of the lipoprotein sample is blotted from the EM grid through a side entrance of the box (**H**), using a spatula covered with filter paper. Blotting of the sample results in the formation of thin films of lipoprotein solution in the holes of the lacey substrate on the EM grid. Upon formation of the thin films, the preparation is equilibrated at the set temperature for an additional 5 min. Subsequently, control switch (**C**) pressurizes the plunger (**B**), which forces the attached forceps through the opened shutter into the container of liquid propane (**I**). Propane

in the central compartment of container (**I**) is kept in a liquid state by liquid nitrogen, present in the outer compartment of container (**I**).

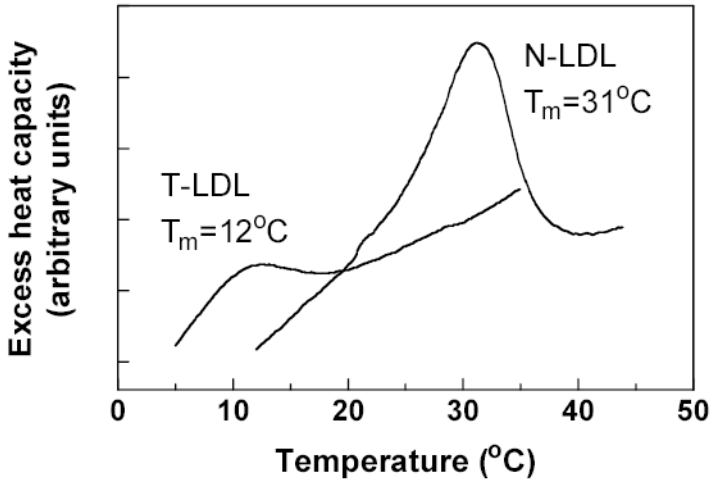

Figure 2.
DSC of N-LDL and T-LDL. Representative thermograms of N-LDL with a high phase-transition temperature (T_m = 31°C) and T-LDL with a low phase-transition temperature (T_m = 12°C) are shown.

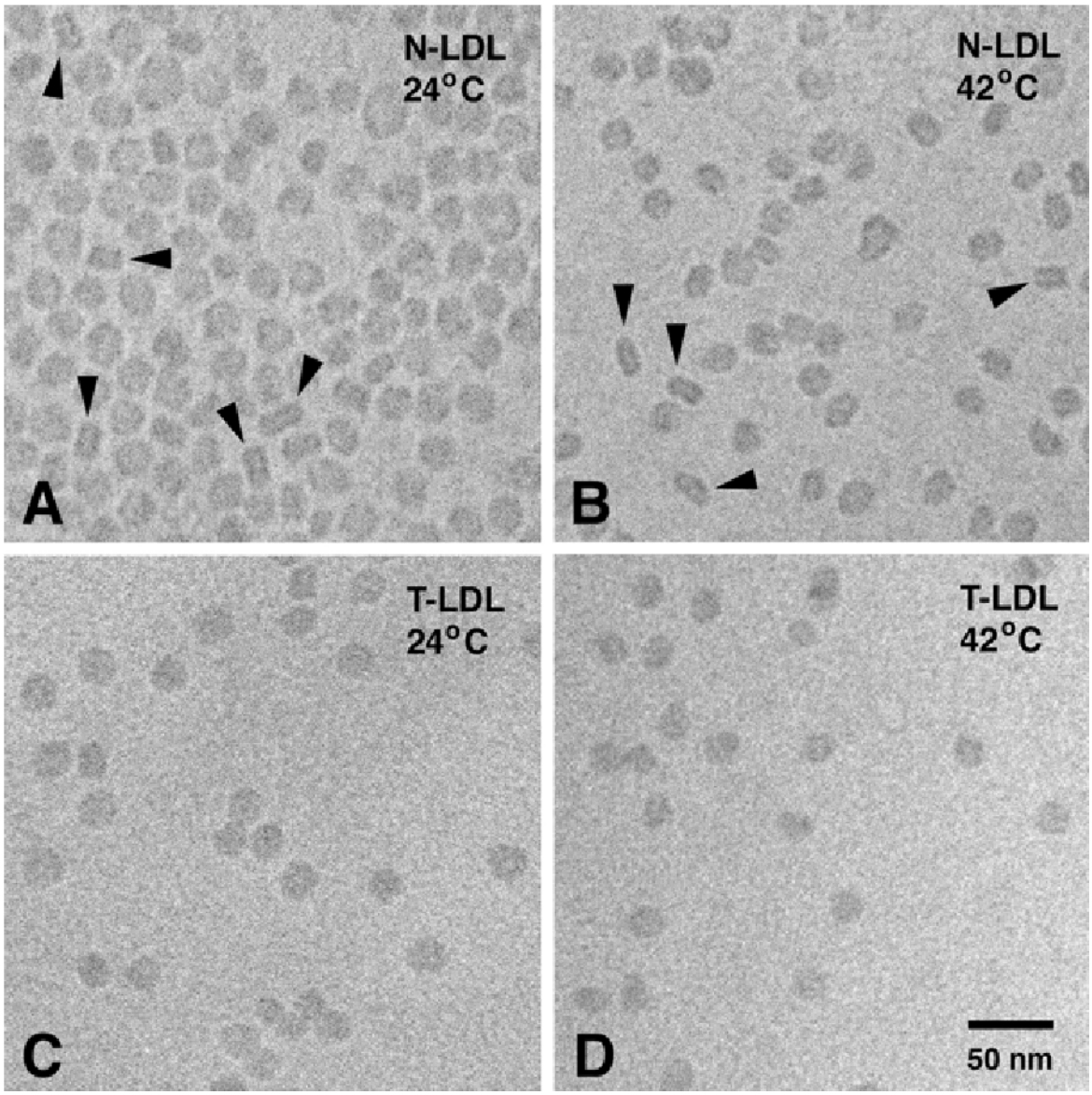

Figure 3.
Cryo-electron micrographs of N-LDL (**A, B**) and T-LDL (**C, D**), ultra-rapidly frozen from 24° C (**A, C**) and 42°C (**B, D**). Arrowheads indicate rectangular projections with two high-density bands, representing edge-on views of the LDL disc (29–31). Magnification 300,000 x.

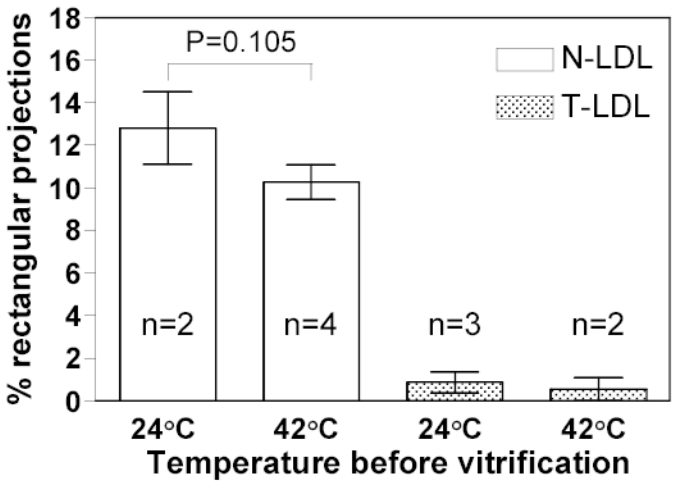

Figure 4.

Frequency distribution of rectangular projections with two high-density bands in cryo-EM preparations of N-LDL and T-LDL, vitrified from 24°C or 42°C. The occurrence of rectangular projections in N-LDL preparations vitrified from 24°C or 42°C is not significantly different (t-test; P=0.105); “n” refers to the number of separate LDL preparations analyzed using cryo-EM.

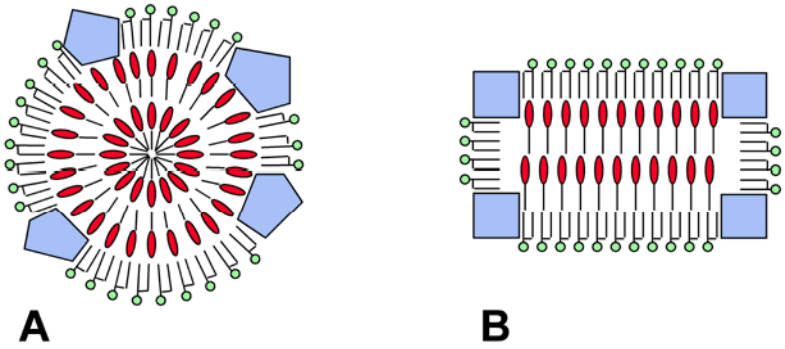

Figure 5.

Highly schematic representations of the liquid-crystalline LDL core (cross-sectional views). &dcl001; Phospholipids; &dcl002; Cholesteryl esters; &dcl003; Apo B. Free cholesterol and triacylglycerols have been omitted from the drawings for clarity **A:** Generalized representation of earlier models (19–25). In these models, the LDL particle is spherical and the liquid-crystalline core is organized in concentric shells of cholesteryl esters. B: Generalized representation of new models (32,35,36), in which the liquid-crystalline core contains flat layers of cholesteryl esters.

Table 1

Properties of normal LDL (N-LDL) and triglyceride-rich LDL (T-LDL).

Chol: total cholesterol; TG: triglycerides; T_m: Midpoint of the phase-transition of the LDL core, determined using DSC; Size of the lipoprotein particles is indicated as the diameter of circular LDL projections in cryo-EM preparations frozen from 24°C. Values are the mean of analyses on three different LDL preparations ± standard error. *Separate experiments have shown that the *in vitro* conversion of N-LDL to T-LDL does not influence the free cholesterol and total phospholipid contents of the lipoprotein particle: The free cholesterol content of N-LDL and T-LDL was 0.35 ± 0.08 mg/mg protein (n=5) and 0.30 ± 0.03 mg/mg protein (n=5), respectively (P=0.128), while the total phospholipid content of N-LDL and T-LDL was 0.82 ± 0.17 mg/mg protein (n=5) and 0.75 ± 0.06 mg/mg protein (n=5), respectively (P=0.379).

	*Chol/Protein (w/w)	TG/Protein (w/w)	*Chol/TG(w/w)	T_m (°C)	Size (nm)
N-LDL	1.34 ± 0.08	0.15 ± 0.05	9.81 ± 2.57	31.1 ± 0.96	19.8 ± 1.85
T-LDL	1.08 ± 0.19	0.30 ± 0.08	3.81 ± 0.73	15.0 ± 1.79	18.5 ± 1.92

Table 2

Core properties and overall shape of normal LDL (N-LDL) and triglyceride-rich LDL (T-LDL).

T_m: Midpoint of the phase-transition of the LDL core, determined using DSC. Indicated are the physical state of the LDL core, and the overall shape of the lipoprotein particle, as observed in cryo-electron micrographs.

	T_m (°C)	Physical State / Shape at 24°C	Physical State / Shape at 42°C
N-LDL	31.1 ± 0.96	Liquid Crystalline / Disk	Liquid / Disk
T-LDL	15.0 ± 1.79	Liquid / Sphere	Liquid / Sphere